Desalination and Water Treatment
www.deswater.com

doi: 10.5004/dwt.2022.28575

264 (2022) 72–90
July

Efficient use of circulating fluidized bed combustion fly ash and slag generated as a result of sewage sludge incineration to remove cadmium ions

Tomasz Kalak

Department of Industrial Products and Packaging Quality, Institute of Quality Science, Poznań University of Economics and Business, Niepodległości 10, 61–875 Poznań, Poland, email: tomasz.kalak@ue.poznan.pl

Received 13 January 2022; Accepted 9 May 2022

ABSTRACT

In a time of globalization, industrial and economic development, new technologies, and pollution of the natural environment have become serious global problem. Due to the superior role of water in maintaining life on Earth, ensuring its purity seems to be a key issue. Heavy metals seem to be one of the most harmful pollutants in the natural environment. For this reason, there are indications to look for new and cheap methods of removing metal ions from wastewater and the aquatic environment. In these research studies, fly ash and slag obtained in circulating fluidized bed combustion technology were used to analyze the adsorption processes of Cd(II) ions. The physical and chemical properties of adsorbents were characterized, such as granulation analysis, bulk density, particle size composition, scanning electron microscopy-energy-dispersive X-ray spectroscopy elemental analysis, thermogravimetry, Brunauer–Emmett–Teller adsorption and desorption, pore-volume, scanning electron microscopy and transmission electron microscopy image analysis, Fourier-transform infrared spectroscopy. The results of the experiments showed high adsorption efficiency and adsorptive capacity of Cd(II) ions on the adsorbents tested. It can be concluded that the obtained results are a sufficient impulse to continue research in this area. Industrial waste in the form of fly ash and slag could be successfully used in adsorption processes to remove Cd(II) ions from wastewater.

Keywords: Water quality; Sewage sludge; Fly ash and slag waste; Circulating fluidized bed combustion technology; Adsorption processes; Cd(II) ions

1. Introduction

The main causes of contemporary pollution of the natural environment include mainly economic development, industrialization, overproduction and consumerism. Despite the large civilization development, universal access to knowledge or research, reducing environmental pollution or cleaning remains a challenge for many countries around the world. Heavy metals are one of the greatest dangers that most often end up with industrial wastewater in lakes, rivers, seas and oceans. In this way, they get into the food chain and spread uncontrolled in nature, causing havoc in living organisms [1,2]. According to the World Health Organization (WHO), Cd, Cr, Cu, Pb, Hg and Ni are the most toxic metals [3]. They come from various industries such as chemical, petrochemical, fertilizer, electroplating, paper tanning and others. Bioaccumulation of metals in human tissues and organs can cause many serious health problems, such as brain damage, organ tumors, cardiovascular diseases, respiratory and nervous system diseases and many others [4,5].

The removal of heavy metals from the aquatic environment can be realized using many techniques, such as electrochemical methods, ion exchange, chemical precipitation and membrane techniques. Another method is the process of metal ion adsorption on various adsorbents,

which is promising due to many advantages, such as ease of implementation of the process, the applicability of a batch system, process continuity, low concentration application, regeneration and reuse of adsorbents as well as low process costs [6]. Well-known and frequently used sorbents include activated carbon, silica gels, zeolites, ion exchange resins, materials synthesized from zeolites, aluminosilicate minerals, or graphene oxides. They are able to achieve high ion binding efficiency, however, their main disadvantage is high production costs. An alternative solution may be the use of cheap adsorbents obtained from industrial waste, such as sewage sludge, biomass waste from various industries, and combustion products such as slag or fly ash [7].

According to the Central Statistical Office (GUS), in 2014 there were 3,264 municipal sewage treatment plants in Poland and the amount of municipal sewage sludge produced was approximately 540.3 thousand tons [8]. According to statistical data, it is estimated that the amount of municipal sewage sludge increases by about 2%–2.5% each year (in terms of dry weight) [9]. In recent years, there has been a significant increase in interest in the reduction of sewage sludge using the circulating fluidized bed combustion (CFBC) technology. Currently, 11 plants in Poland use the method of thermal conversion of sewage sludge. Seven of them use CFBC technology, while four plants burn the sludge on a grate. The average amount of fly ash generated from sewage sludge is estimated at over 160 thousand tons per year in Poland [10]. The main benefit is a significant reduction in the weight of waste and the products of combustion are fly ash and slag, which are irregular in shape with a porous surface, a high content of dehydrated silicate minerals and other minerals, and a large specific surface area. It is worth noting that the cost of these waste materials is low and they can be reused in the industry in line with the idea of circular economy and sustainable development. Therefore, the search for and subsequent use of industrial waste adsorbents may be important for the removal of toxic pollutants from wastewater in the future [2,11–14].

Cadmium is one of the metals most frequently polluting the aquatic environment. It was selected for this study due to its wide industrial application and negative impact on living organisms. Cadmium occurs naturally in water, air, soil and foodstuffs. The most common form of metal is cadmium sulfide (77.6% Cd), cadmium carbonate (61.5% Cd), and cadmium oxide (87.5% Cd). Cadmium is also present in waste from industrial processes, such as the production of alloys, cadmium-nickel batteries, pesticides, fertilizers, plastics, pigments and dyes, smelting, electroplating, mining, refining and the textile industry [15–17]. Cadmium belongs to the group of metals that are toxic to living organisms and is a big problem for the environment due to its non-degradability. The WHO organization recommends a maximum concentration (MCL) of Cd(II) in drinking water up to 0.005 mg/L [15].

The aim of this study was to determine the physicochemical properties of circulating fluidized bed combustion fly ash (CFBC-FA) and slag (CFBC-S) obtained as a result of sewage sludge incineration using the fluidized bed circulation combustion (CFBC) technology. In addition, the purpose was to determine the adsorption properties in relation to Cd(II) ions as well as to analyze the kinetics of the adsorption process.

2. Process of CFBC-FA and CFBC-S formation

Currently, appropriate waste management is one of the most important challenges faced by the economies of various countries. Bearing in mind the negative impact of waste on the natural environment, there are legislative provisions limiting its storage, suggesting their reuse or weight reduction and disposal in incineration processes.

Sewage sludge incineration becomes an alternative method given the limitations of sewage sludge use due to excessive heavy metal content. Its use is influenced by the chemical composition of sewage sludge and the percentage of flammable substances. The use of heat with energy recovery is currently the most effective and the best method of sewage sludge disposal due to environmental protection and energy savings [18]. The most important benefit is that weight of waste is significantly reduced. Other additional benefits include energy use of sewage waste, system stability, low susceptibility to changes in the composition of waste, minimization of odors, and the possibility of using fly ash as a filter material or as an additive to concrete, asphalt, bricks and hollow blocks production. The main limitation is the production of by-products, the quantity and quality of which depend on the chemical composition of the sludge, combustion conditions and exhaust gas treatment technology. In addition, other constraints are the high construction costs of the incineration plant and the high operating costs [19]. The most technologically advanced design solution seems to be the CFBC technology. The main advantages include compatibility with a wide range of fuels (gas, oil, high-grade and low-grade coal, biomass, sewage sludge, waste plastics, used tires), low pollution, high efficiency of the combustion process and energy efficiency, the possibility of simultaneous combustion of dehydrated and dried and fermented sludge and the ease of maintenance of the installation [20].

The process of CFBC-FA and CFBC-S formation in the CFBC technology is schematically shown in Fig. 1. In this process, the sewage sludge mixture is transported for drying using a piston pump in order to evaporate water. Water vapor in the dryer is condensed and transported to the sewage treatment plant. The dried sludge containing about 33% dry weight is fed to the fluidized bed kiln using a system of feeders. The layer of sand at the bottom of the furnace is lifted by heated air fed through nozzles during the combustion process, forming a fluidized bed. In the center of the furnace, starter burners are used to start the furnace and heat the fluidized bed to a temperature of 650°C, which allows sewage sludge to be fed into the furnace. The process exhaust gases are directed to the top of the furnace, where they remain for at least 2 s at a minimum temperature of 850°C. In the fluidized bed furnace, waste gases and slag are produced as a result of burning wastewater. All organic matter present in the sediment is burned in this process. Flue gas is then cooled and cleaned, and heat from its cooling heats the air needed to fluidize the bed. The cooled gases are either dry or wet treated. They are already pre-treated in a fluidized bed where limestone is added, which reacts with NOx,

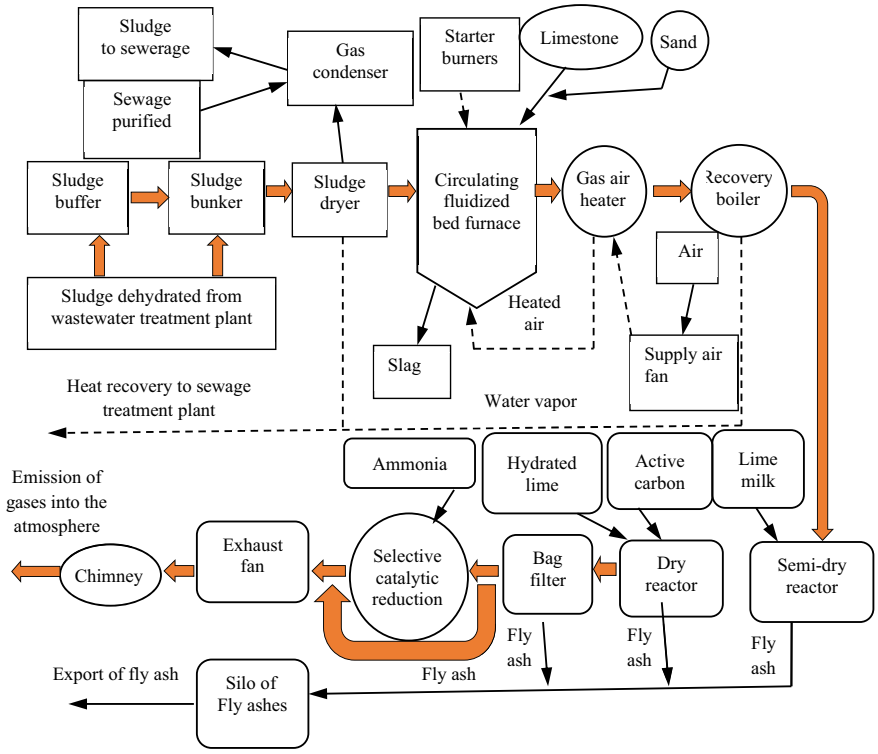

Fig. 1. Schematic diagram of the sewage sludge utilization process and fly ash (CFBC-FA) and slag (CFBC-S) formation using CFBC technology.

SOx, chlorine and fluorine to form calcium compounds. The removal of acid components of the off-gas takes place in a semi-dry reactor fed with lime and compressed air. The waste gases are transported to a dry reactor in which lime and activated carbon bind dioxins, furans and heavy metals. The final removal of pollutants from the exhaust gases takes place in a bag filter where fly ashes are retained. They are deposited on the outer surface of the bags and then thrown into the conical part of the tank, from where they are transported to the silo. In the final stage, the cleaned flue gases are directed to the chimney and to the atmosphere.

It is estimated that about 20%–25% of municipal solid waste generated in the European Union is thermally transformed in incineration processes. The number of installations dedicated to waste incineration in the EU is over 400 and the average weight of incinerated municipal solid waste is equal to about 200,000 tons/y. There are several mono-incineration plants in Poland placed in the following locations: Szczecin, Gdynia, Gdańsk, Olsztyn, Warsaw, Bydgoszcz, Łódź, Zielona Góra, Kielce, Łomża, and Cracow [21].

3. Experimental procedure

3.1. Materials and methods

3.1.1. Preparation of research samples

Fly ash and slag used in this study were obtained in one of the sewage treatment plants in Poland as a result of the CFBC technology. The samples were taken from the fluidized bed and prepared in accordance with Polish standards PN-EN 14899:2006 and PN-EN 15002:2006. The samples were dried at 105°C to constant weight (<0.2% humidity). All chemicals were pure for analysis and distilled water was used in the experiments.

3.1.2. CFBC-FA and CFBC-S characterization

CFBC-FA and CFBC-S particles with a diameter less than 0.212 mm were used in these research studies. Physicochemical properties of the samples were examined using the following techniques: granulation analysis, particle size distribution, bulk density, the elemental composition using scanning electron microscopy-energy-dispersive X-ray spectroscopy (SEM-EDS) analysis, thermogravimetry, specific surface area and mean pore diameter Brunauer–Emmett–Teller (BET), pore volume Barrett–Joyner–Halenda (BJH), SEM and transmission electron microscopy (TEM) analysis, Fourier-transform infrared spectroscopy (FTIR). These research methods and apparatus have been characterized and listed with supplementary information.

3.1.3. Cd(II) sorption experiments

Determination of the efficiency of the Cd(II) ions removal process on CFBC-FA and CFBC-S was carried out in batch experiments. $CdCl_2$ (1 g/L standard solution for AAS, Sigma-Aldrich (Germany)) was used in the research. The adsorbent (0.25–25 g/L) and the solution (20 mL) containing metal ions were placed in a 50 mL conical flask and shaken at 150 rpm for 1 h until equilibrium was reached. The initial pH of the stock solutions was adjusted with 0.1 M HCl and NaOH. Then, adsorption solutions were centrifuged

for 15 min (4,000 rpm) for phase separation. The concentration of metal ions was analyzed using atomic absorption spectrophotometry (F-AAS, wavelength λ = 228.8 nm for cadmium, SpectrAA 800 (Varian, Palo Alto, USA)). Measurements were carried out in triplicate at room temperature (23°C ± 1°C) under normal pressure and the results are presented as mean values. Adsorption efficiency R (%) and adsorption capacity q_e (mg/g) were calculated according to Eqs. (1) and (2), respectively:

$$R = \left[\frac{C_0 - C_e}{C_0}\right] \times 100\% \quad (1)$$

$$q_e = \frac{\left(C_0 - C_e\right) \times V}{m} \quad (2)$$

where C_0 and C_e are initial and equilibrium Cd(II) ion concentrations (mg/L), respectively; V is the volume of solution (L) and m is the mass of blackberry biomass (g).

Kinetic and isothermal studies were performed using pseudo-first-order and pseudo-second-order, Langmuir and Freundlich's models based on Eqs. (3)–(6), respectively:

$$q_t = q_e\left(1 - e^{k_1 t}\right) \quad (3)$$

$$q_t = \frac{q_e^2 k_2 t}{1 + q_e k_2 t} \quad (4)$$

$$q_e = \frac{q_{\max} K_L C_e}{1 + K_L C_e} \quad (5)$$

$$q_e = K_F C_e^{1/n} \quad (6)$$

where q_t is the amount of Cd(II) ions adsorbed (mg/g) at any time t (min); q_e is the maximum amount of Cd(II) ions adsorbed per mass of the biosorbent (mg/g) at equilibrium; k_1 is the rate constant of pseudo-first-order adsorption (1/min); k_2 is the rate constant of pseudo-second-order adsorption (g/(mg min)); $q_{\max}$ is the maximum adsorption capacity (mg/g); K_L is the Langmuir constant; C_e is the equilibrium concentration after the adsorption process (mg/L); K_F is the Freundlich constant and $1/n$ is the intensity of adsorption.

4. Results and discussion

4.1. Characterization of the materials

Granulation analysis showed the following results: (a) distribution of CFBC-FA particles: 0–0.212 mm – 87.6%; 0.212–0.500 mm – 11.4%; 0.500–1.0 mm – 1.0%; (b) distribution of CFBC-S particles: 0–0.212 mm – 12.9%; 0.212–0.5 mm – 73.7%; 0.500–1.0 mm – 11.3%; 1.0–1.7 mm – 0.49%; >1.7 mm – 1.61%. The studies have shown that the particles are not homogeneous and their size has a significant impact on the adsorption process. According to the literature, the smaller particle size of fly ash and slag, which is associated with the larger specific surface area and the number of active centers, favors higher efficiency of metal ions adsorption [22–25]. Hence, for this reason, the smallest fractions with a diameter of less than 0.212 mm were used in the experiments.

Based on the analysis of particle size distribution using laser diffraction, only one peak was found at the particle size of 1,206 and 956.3 nm for CFBC-FA and CFBC-S, respectively (Figs. S1 and S2). The limitation of the study was that not all particles were able to form a suspension in the aqueous solution, heavier and larger particles fell to the bottom of the solution. Therefore, it was only possible to analyze the particles suspended in the solution. The difference is that CFBC-FA particles are more volatile and less dense compared to slag.

Bulk density was determined by loosely pouring samples into a cylinder and compacting them on a vibrating table. The following results were obtained: 0.74 ± 0.01 g/cm^3 and 1.49 ± 0.02 g/cm^3 for CFBC-FA, respectively. In case of CFBC-S, the results are as follows: 0.83 ± 0.02 and 1.34 ± 0.02 g/cm^3, respectively. As a result of the compaction process, the bulk density of both materials increased.

The results of elemental analysis using the SEM-EDS method are presented in Table 1 and Figs. S3 and S4. CFBC-FA mainly contains such elements as O, Ca, P, Al, Si, Fe, Mg and oxides of CaO, P_2O_5, Al_2O_3, SiO_2, Fe_2O_3, CO_2, MgO. In turn, slag consists mainly of Ca, O, Fe, S, P, Al, Si, C and CaO, SO_3, Fe_2O_3, P_2O_5, SiO_2, CO_2, Al_2O_3. A characteristic feature of this method is the fact that the measurement is performed pointwise on the surface of the sample. Hence, bearing in mind the complexity of CFBC-FA and CFBC-S samples, quantitative and qualitative composition may slightly differ in different places of agglomerates composed of various particles depending on the location of the measuring point.

Table 1
Elemental composition of CFBC-FA and CFBC-S (SEM-EDS analysis)

Elements	C	O	Na	Mg	Al	Si	P	S	K	Ca	Ti	Mn	Fe	Zn
CFBC-FA (%), weight	1.85	44.8	0.54	3.28	6.41	5.51	11.3	0.41	1.11	17.7	0.54	0.23	5.43	0.87
CFBC-FA (%), atomic	3.41	61.9	0.52	2.99	5.25	4.34	8.11	0.28	0.63	9.76	0.25	0.09	2.15	0.29
CFBC-S (%), weight	1.19	36.5	0.27	1.0	1.92	1.98	2.47	4.59	0.13	37.9	0.44	–	7.84	–
CFBC-S (%), atomic	2.46	56.9	0.3	1.03	1.78	1.76	1.99	3.58	0.08	23.6	0.21	–	3.51	–
Oxides	CO_2		Na_2O	MgO	Al_2O_3	SiO_2	P_2O_5	SO_3	K_2O	CaO	TiO_2	MnO	Fe_2O_3	ZnO
CFBC-FA (%)	6.79		0.73	5.44	12.1	11.8	26.02	1.02	1.3	24.7	0.89	0.29	7.8	1.1
CFBC-S (%)	4.34		0.37	1.66	3.64	4.24	5.65	11.5	0.16	53.1	0.73	–	11.2	–

Thermogravimetric analysis (TGA) was performed and the results are included in the supplementary information (Figs. S5 and S6). It was shown that a weight loss of the samples occurred with increasing temperature. For both materials, the initial weight loss was observed at a temperature ranging from about 30°C to 600°C. In the case of CFBC-FA, a steady linear decrease was demonstrated. Possibly evaporation of water and other volatile substances (e.g., carbon monoxide and/or other organic compounds) took place in this range. In the case of CFBC-S, rapid weight loss in the temperature range of 400°C–460°C occurred. It is likely that the combustion of organic substances present in the sample may have contributed to this change [26]. Another increase in temperature to about 540°C–600°C caused a slight weight decrease of about 0.6%. This phenomenon may be related to the release of gases from the inside of grains as a result of the destruction of their surface walls. As a result of a derivative weight loss analysis (DTG), two peaks at 342°C (CFBC-FA) and 421°C (CFBC-S) are shown, which is probably related to the dehydroxylation of calcium hydroxide. At around 600°C, another decrease in DTG was recorded, which may be due to gas evaporation [27].

Based on the BET and BJH analysis, for CFBC-FA and CFBC-S specific surface area is 3.75 and 1.87 m^2/g, pore volume (V_p) is 0.014 and 0.0096 cm^3/g and mean pore diameter (A_{pd}) is 17.6 and 21.2 nm, respectively (Figs. S7–S14). Adsorption isotherms are different and depend on the size of pores and intensity of interaction of Cd(II) ions with adsorbents. It is assumed that their shape is similar to type III isotherms, which informs about cooperative adsorption, meaning that previously adsorbed particles can lead to increased sorption of other remaining particles. Low adsorption efficiency may occur in the case of low relative pressure and weak interaction between metal ions and adsorbents. However, the interaction of metal ions with adsorbents has a positive effect on the adsorption of other remaining metal ions in a situation where the ions have already been adsorbed at least once, the consequence is bulging of the isotherm towards the pressure axis [28,37].

SEM images of CFBC-FA and CFBC-S particles are shown in Fig. 2. Based on the analysis, it can be assumed that the particles are compact and spongy, have irregular shapes and structures and a porous surface. Larger particles show more irregularity than smaller ones. The temperature and time of the combustion process contribute to the irregular shape of the particles. The longer the process, the more spherical or crystalline the particles [29]. Several literature publications state that parameters such as combustion time and temperature have an influence on the formation of the shape of fly ashes and slags. The particles can take acicular, elongated or irregular forms, and as a result of extended burning time, they can be spherical or crystalline [30,31]. Fig. 3 shows TEM images of the research samples. The presence of flocs of various sizes and irregular shapes (amorphous structure) was found. The particles have different shades, the darker zones are the thicker the layers of material, and the lighter zones are the thinner layers of the material. No opaque parts were observed. Similar observations are presented by other authors in the literature [32–34].

FTIR analysis of CFBC-FA and CFBC-S was carried out and the spectra are presented in Fig. S15. On the basis of comparative analysis of the peaks with standard absorption frequencies of functional groups, functional bonds and types of vibrations occurring in the examined samples were characterized. Among them the following peaks have been found: bond bending vibrations Si–O–Si (391, 397, 406, 407, 415, and 457 cm^{-1}) [38], O–P–O, O=P–O bending vibration (probably phosphorus pentoxide, 553 cm^{-1}), vibrations Si–O–M (M – metal, 593, 596 cm^{-1}), stretching vibrations Al–O [37], symmetric stretching of Al–O–M [25], the vibration of carbonates (calcite, 875 cm^{-1}), asymmetric stretching vibrations of silica Si–O–Si and Al–O–Si (1,027 and 114 cm^{-1}), valence vibration of carbonate ions, C=C stretching bond in aromatics (1,422–1,424 cm^{-1}), asymmetric and symmetric stretching vibrations O–H (hydrated aluminum silicates or amorphous silicates, 3,642–3,644 cm^{-1}) [35]. Analogous results of the FTIR analysis have been reported in the literature [36–38].

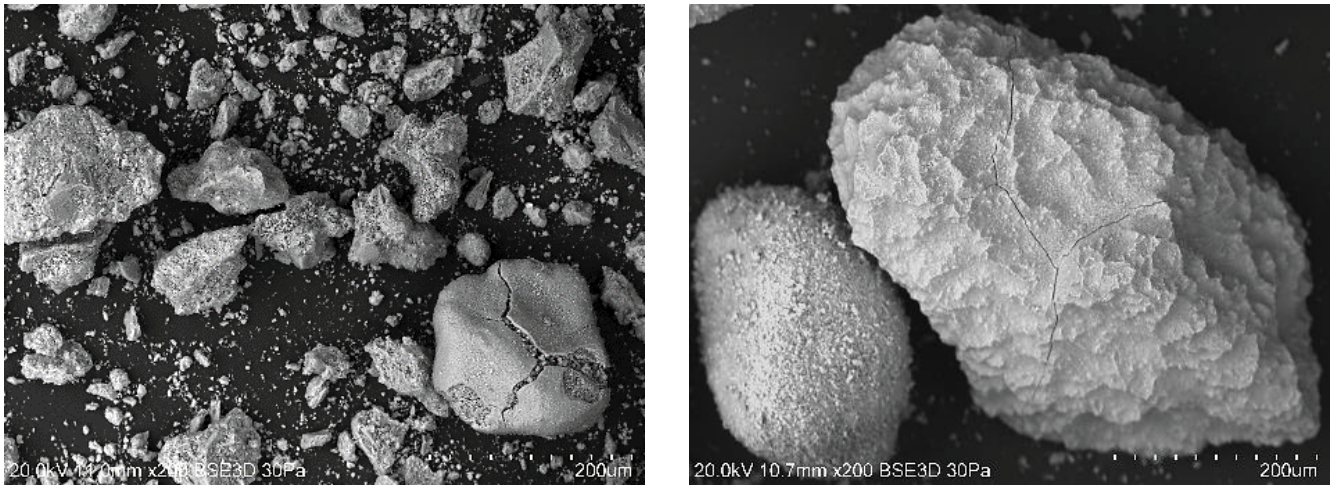

(a) (b)

Fig. 2. SEM images of CFBC-FA (a) and CFBC-S (b) (Magn.: x200, scale bar: 200 μm).

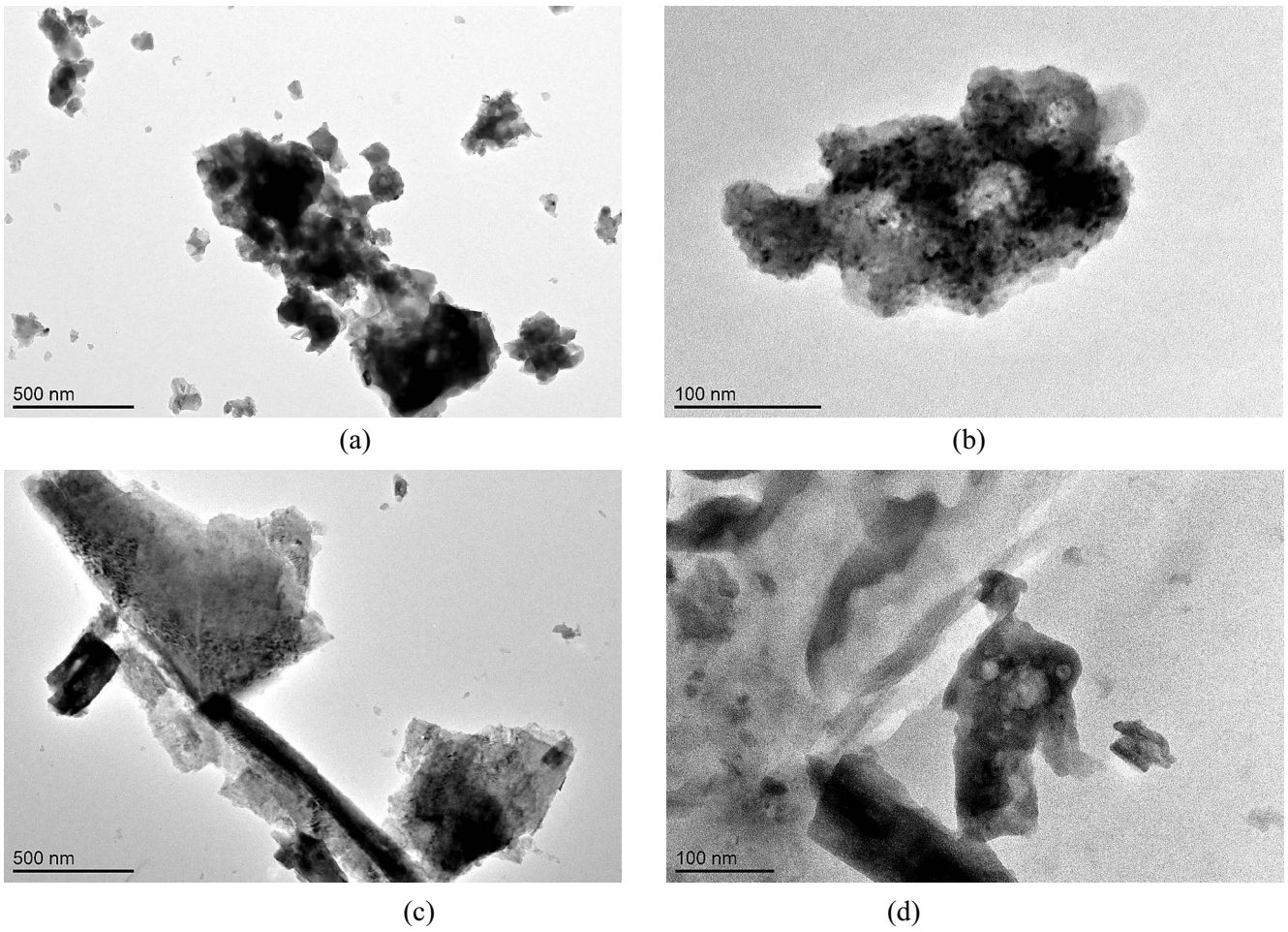

Fig. 3. TEM images of CFBC-FA: (a) scale bar: 500 nm, (b) 100 nm, and CFBC-S: (c) 500 nm, (d) 100 nm.

4.2. Adsorption studies

4.2.1. Impact of initial pH

In these studies, the effect of initial pH on the adsorption efficiency was examined and the results are presented in Figs 4 and 5. The experiments were performed under the following conditions: initial concentration of Cd(II) ions 100.1 mg/L, adsorbent dosage 1–3 g/L, initial pH range of 2–5, contact time 60 min, T = 23°C, agitation speed 200 rpm. As it is seen in Figs. 4 and 5, the highest sorption efficiency was achieved at initial pH 4.0 for the adsorbent doses of 1 g/L (81.14%), 3 g/L (84.93%), 5 g/L (95.87%) for CFBC-FA, and 1 g/L (70.98%), 3 g/L (76.6%), 5 g/L (93.54%) for CFBC-S. At initial pH 2.0, the lowest adsorption efficiency in the range of 10%–20% was observed. Thereafter, with an increase in initial pH, the efficiency of the process also increased. In order to discuss the relationship between the initial pH of the solution and adsorption, the surface charge of CFBC-FA and CFBC-S as well as the degree of speciation should be considered. The examined adsorbents are basic in nature, therefore their addition increases the pH of the solution during the processes. The presence of such anions in the adsorbent material as OH^-, SO_4^{2-}, CO_3^{2-}, PO_4^{3-}, and SiO_3^{2-} could contribute to the precipitation of cadmium

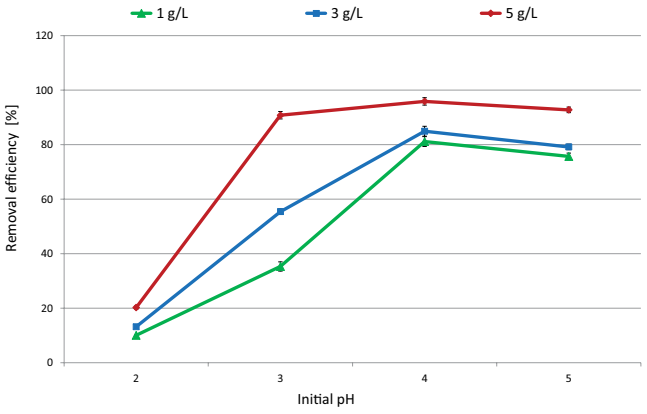

Fig. 4. Impact of initial pH on the Cd(II) adsorption efficiency (CFBC-FA dosage 1–5 g/L).

ions from the solution at higher pH. The pH parameter influences the electrostatic charge of metal oxides, the content of which is high in these adsorbents. Hence, the process of binding Cd(II) ions may result from ion exchange and/or complexation through bonding with oxygen groups. The mechanism reactions can be proposed as follows:

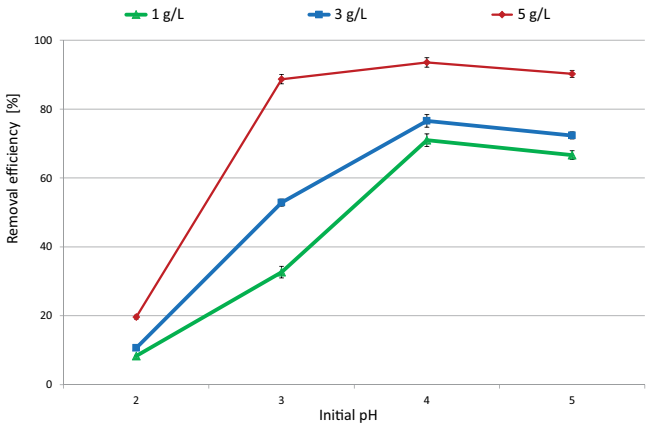

Fig. 5. Impact of initial pH on the Cd(II) adsorption efficiency (CFBC-S dosage 1–5 g/L).

$$-XOH + H_3O^+ \rightarrow XOH_2^+ + H_2O \quad (7)$$

$$-XOH + OH^- \rightarrow XO^- + H_2O \quad (8)$$

$$2\left(-XO^-\right) + Cd^{2+} \rightarrow \left(-XO\right)_2 Cd \quad (9)$$

where X can be represented by K, Si, Al, Ca, etc. It should be noted that the proposed mechanism was not confirmed by additional experiments in this research [2,39].

During the adsorption processes, the hydrated surface of the adsorbents could be protonated by a significant amount of hydrogen ions ($MOH + H^+ \rightarrow M(OH)_2^+$). The result was a reduction in the number of negatively charged particles and at the same time an increase in the number of positively charged active centers. In alkaline solutions, hydroxide ions react with hydrated oxides, resulting in the formation of deprotonated ions ($MOH + OH^- \rightarrow MO^- + H_2O$). In acidic solutions, cadmium takes Cd^{2+} ionic form, which allows competing with H^+ ions. As a result, electrostatic repulsion occurs which is not favorable for binding positively charged cadmium ions, resulting in lower adsorption efficiency. When initial pH was increased to 3 and 4, the surface of the adsorbents became more negatively electrostatically charged, the groups were properly deprotonated as a result of ion exchange, which resulted in greater adsorption of Cd^{2+} ions. Additionally, increased dissociation of surface hydroxyl groups from adsorbent surfaces may contribute to the improvement of the process efficiency [2,39].

4.2.2. Impact of sorbent dosage

The effect of CFBC-FA and CFBC-S dosage on Cd(II) adsorption is shown in Figs. 6 and 7. The experiments were performed under the following conditions: initial concentration of Cd(II) ions 102.4 mg/L, initial pH 3.9, T = 23°C, contact time 60 min. It was shown that when the adsorbent dose was increased up to 5 g/L, process efficiency also increased sharply to 97.9% (CFBC-FA) and 98.1% (CFBC-S). As it is seen, the adsorbent dosage of 5 g/L can be

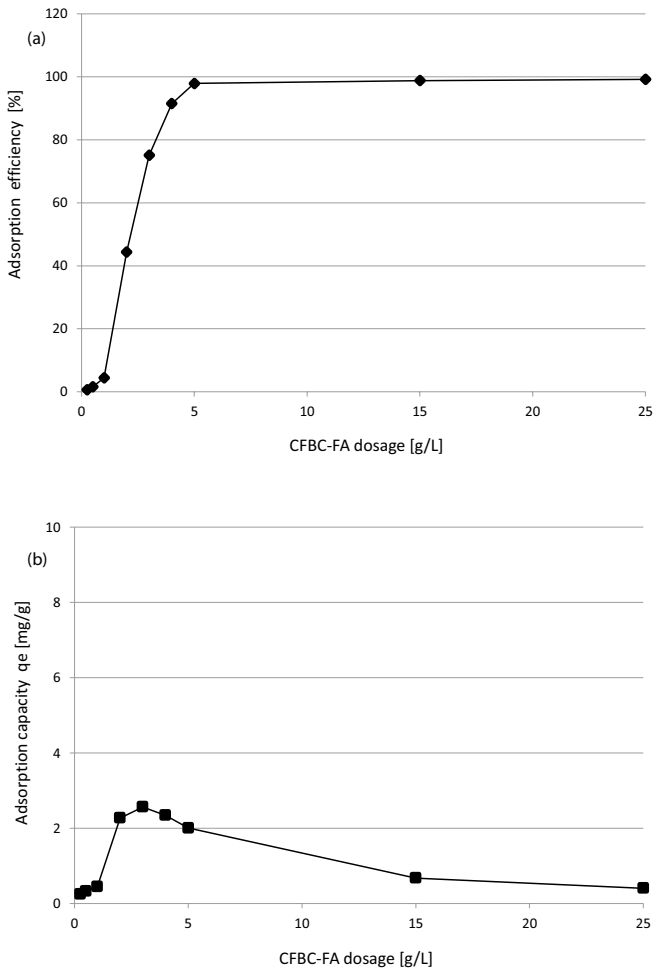

Fig. 6. Effect of CFBC-FA dosage on Cd(II) (a) adsorption efficiency and (b) adsorption capacity.

considered optimal, because further increasing the mass of adsorbents did not cause a significant change and the process efficiency remained at the same high level. Moreover, experimental adsorption capacity increased up to 2.5 mg/g (CFBC-FA) and 2.7 mg/g (CFBC-S) at dosage of 3 g/L, and then slowly decreased to 0.4 mg/g (25 g/L). The sudden increase in the first phase is related to the most active stage of the adsorption process, where all free active sites are filled with cadmium ions. Active centers available for further adsorption were not fully used with greater dosages of adsorbents. Therefore, a gradual decrease in the adsorption capacity was noticed [29].

4.2.3. Impact of initial concentration of Cd(II) ions

The study of the effect of different initial concentrations of Cd(II) ions on adsorption is shown in Figs. 8 and 9. Based on the previous research results, the following experimental conditions were used: initial concentration of Cd(II) (2.5–100 mg/L), adsorbent dosage 1–5 g/L, initial pH 4, contact time 60 min, agitation speed 200 rpm, T = 23°C. Overall, an increase in process efficiency was noted. As it is shown in the figures, the best results, equal

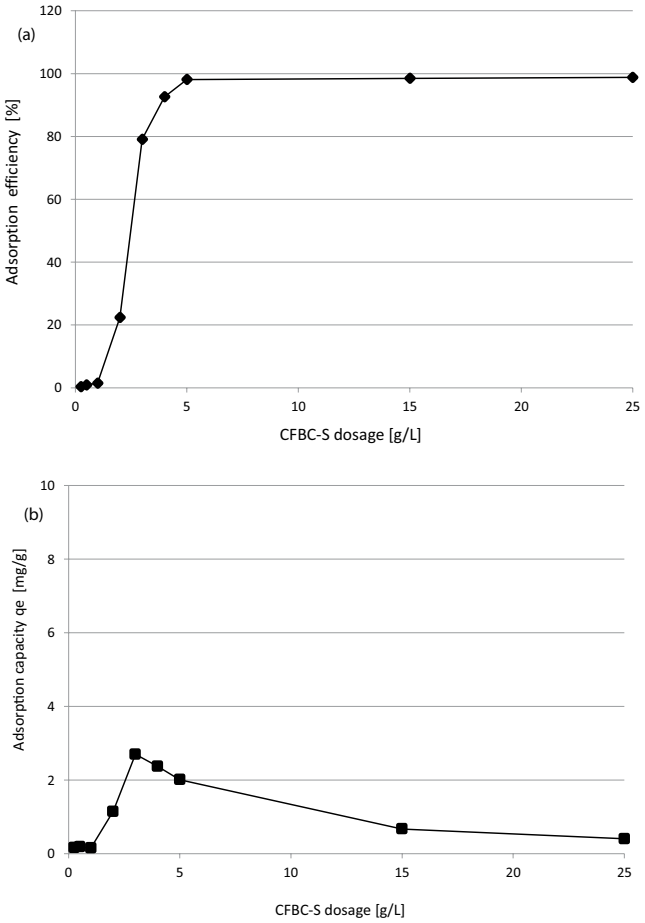

Fig. 7. Effect of CFBC-S dosage on Cd(II) (a) adsorption efficiency and (b) adsorption capacity.

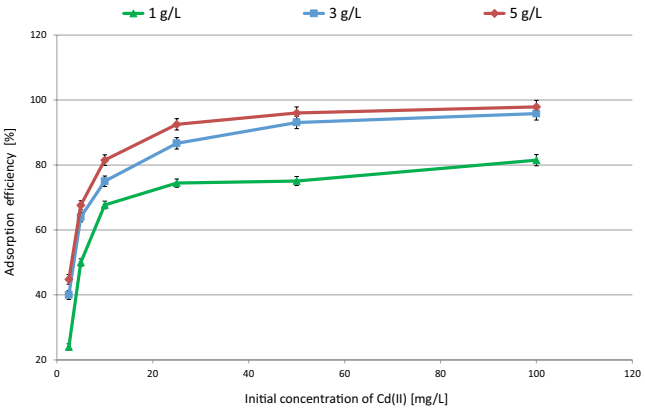

Fig. 8. Impact of initial concentration on the Cd(II) ions adsorption efficiency (CFBC-FA dosage 1–5 g/L).

to 97.9% (CFBC-FA) and 94.9% (CFBC-S), were obtained for a 5 g/L adsorbent dosage and initial concentration of 100 mg/L. The present research results indicated that the initial concentration of cadmium ions in the solution influences the surface saturation of the adsorbent materials. initial concentration in the range of 2.5–10 mg/L was enough for ion exchange at the interface to occur. Based

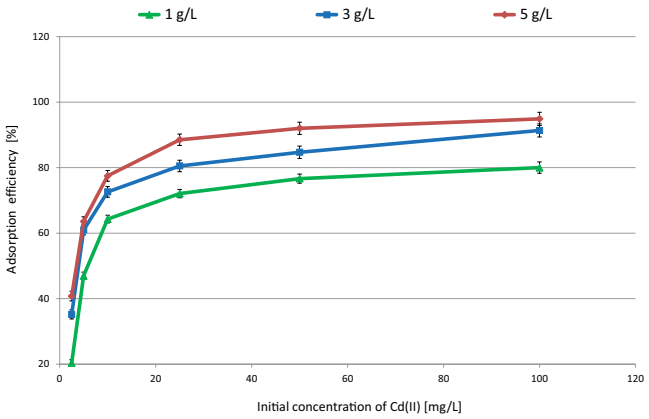

Fig. 9. Impact of initial concentration on the Cd(II) ions adsorption efficiency (CFBC-S dosage 1–5 g/L).

on the literature, the ion radius of Cd^{2+} cation is 97 pm. There is a dependence that a greater tendency to hydrolysis in aqueous solutions occurs with metal ions with smaller ion radii. Hydrolyzed particles of large diameter are characterized by a lower adsorption capacity, which means a lower efficiency of the removal process [40–42].

4.3. Adsorption kinetics

4.3.1. Impact of contact time

The results of the research on the effect of contact time on adsorption efficiency are shown in Figs. 10 and 11. Contact time is an important parameter in research studies on the adsorption process due to the possibility of practical use in industry. Determining optimal contact time may translate into effective process design and industrial implementation, but also into cost reduction. Previous research results in these studies allowed us to establish the following experimental conditions: initial concentration of Cd(II) 100 mg/L, initial pH 4.0, adsorbent dosage 1–5 g/L, T = 23°C, agitation speed 200 rpm. As it is shown in the figures, the maximum adsorption efficiency level of 95.2% (CFBC-FA) and 92.5% (CFBC-S) was achieved in the first 30 min of the process and there were no significant changes up to 60 min, hence there was no need to extend the processing time. An initial increase in adsorption could be the result of a high concentration of Cd(II) ions at the interface and the availability of a larger number of free active sites on the adsorbent surface. The equilibrium of this process was achieved gradually through the occupation of active centers by cadmium ions.

4.3.2. Studies of kinetic models

The pseudo-first-order and pseudo-second-order reaction model was applied to describe the kinetics of Cd(II) adsorption on CFBC-FA and CFBC-S. Calculation parameters (reaction rate constant k, equilibrium adsorption capacity q_e and correlation coefficients R^2) are presented in Table 2 and the isotherms in Figs. 12–15. Based on the calculations, it was shown that higher R^2 coefficients for both adsorbents were observed in the pseudo-second-order model, so

there is a higher correlation between the calculated value of capacity q_t and the experimental value q_e. Therefore, it can be concluded that the pseudo-second-order model best describes the kinetics of Cd(II) adsorption. There is a probability that chemical bonds (chemisorption) were formed and that adhesion to the surface of materials took place during sorption processes. Additionally, in the case of a lower concentration of Cd(II) ions in the solution, particle collisions are less likely to occur [43].

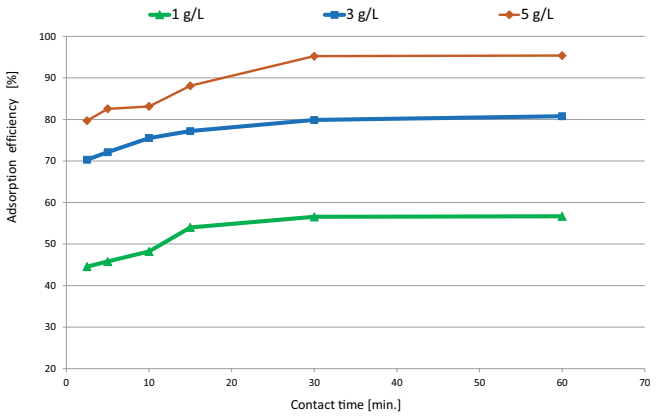

Fig. 10. Impact of contact time on the Cd(II) ions adsorption efficiency (CFBC-FA dosage 1–5 g/L).

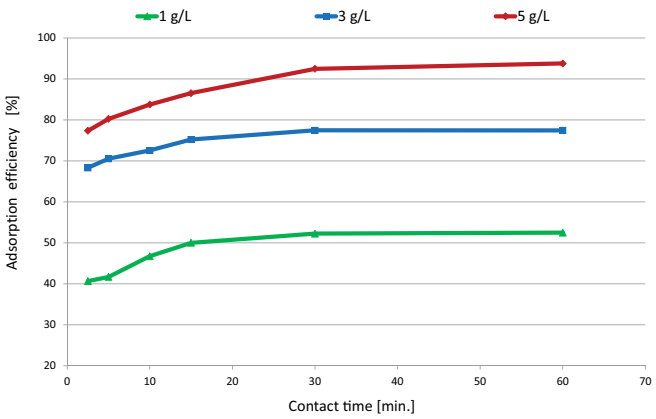

Fig. 11. Impact of contact time on the Cd(II) ions adsorption efficiency (CFBC-S dosage 1–5 g/L).

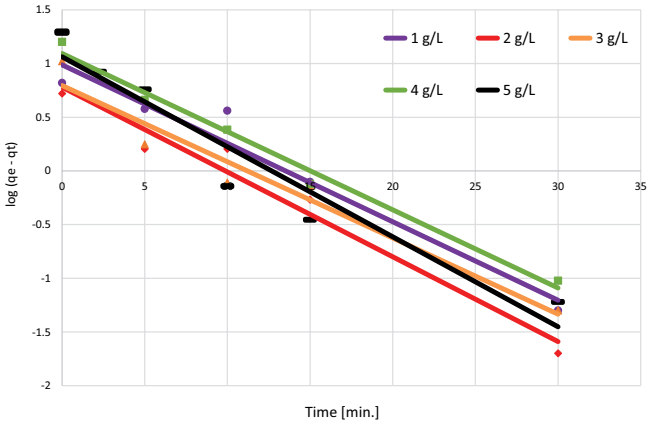

Fig. 12. Pseudo-first-order adsorption isotherms (CFBC-FA dosage 1–5 g/L).

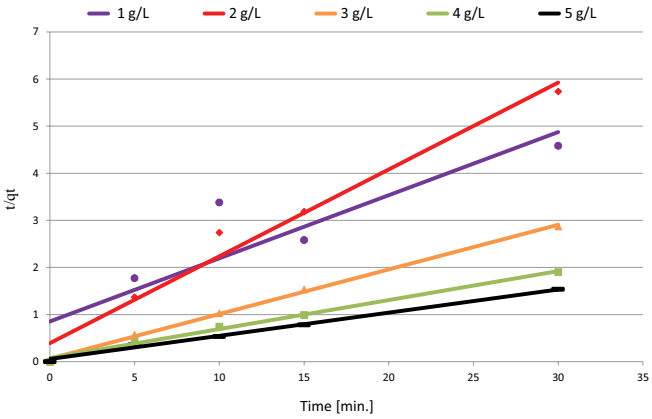

Fig. 13. Pseudo-second-order adsorption isotherms (CFBC-FA dosage 1–5 g/L).

Table 2
Kinetic parameters of pseudo-first-order and pseudo-second-order models

Adsorbent	Adsorbent dosage (g/L)	Pseudo-first-order kinetic model			Pseudo-second-order kinetic model		
		k_{ad} (min^{-1})	q_e (mg/g)	R^2	k (g/mg min)	q_e (mg/g)	R^2
CFBC-FA	1	0.168	9.72	0.955	0.086	7.463	0.801
	2	0.182	6.03	0.967	0.163	5.423	0.976
	3	0.169	6.42	0.953	0.043	10.55	0.998
	4	0.166	12.27	0.986	0.018	16.247	0.994
	5	0.195	11.68	0.933	0.012	20.34	0.994
CFBC-S	1	0.224	39.30	0.946	0.0008	78.07	0.999
	2	0.170	5.48	0.979	0.162	5.434	0.977
	3	0.184	7.96	0.972	0.043	10.59	0.997
	4	0.152	11.78	0.976	0.018	16.22	0.993
	5	0.255	14.76	0.984	0.012	19.89	0.996

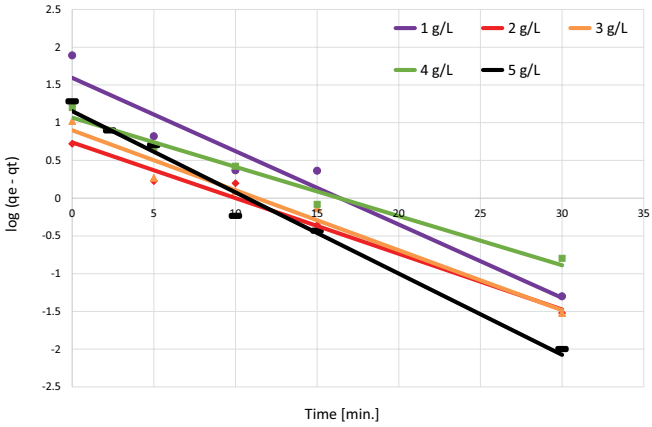

Fig. 14. Pseudo-first-order adsorption isotherms (CFBC-S dosage 1–5 g/L).

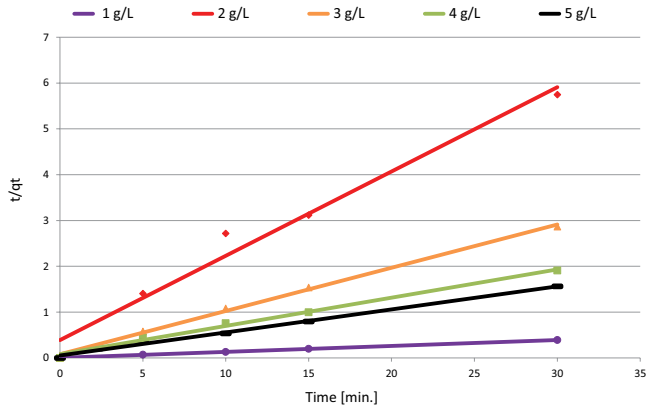

Fig. 15. Pseudo-second-order adsorption isotherms (CFBC-S dosage 1–5 g/L).

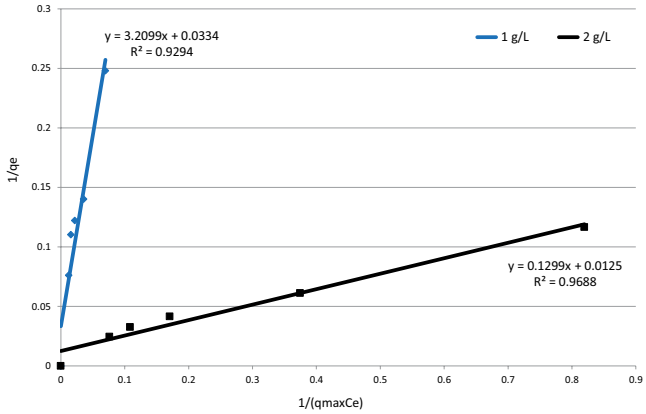

Fig. 16. Langmuir model adsorption isotherms (CFBC-FA dosage 1–2 g/L).

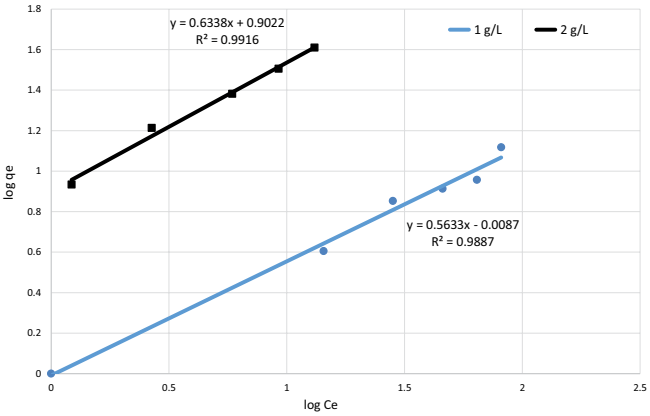

Fig. 17. Freundlich model adsorption isotherms (CFBC-FA dosage 1–2 g/L).

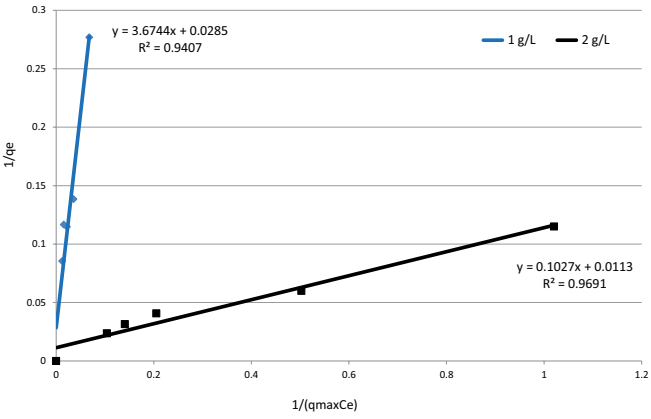

Fig. 18. Langmuir model adsorption isotherms (CFBC-S dosage 1–2 g/L).

4.4. Analysis of isotherm models

Langmuir and Freundlich isotherm models were used to describe the adsorption process of cadmium ions (Figs. 16–19). The calculated parameters for both models are presented in Table 3. In the case of the Langmuir equation, the values of calculated maximum adsorption capacity q_m are estimated at 53.19 mg/g (CFBC-FA, 2 g/L) and 53.01 mg/g (CFBC-S, 2 g/L), respectively. K_L constant is related to the binding energy of the adsorbent and the solute, which relates to the spontaneity of the adsorption process. In accordance with the literature, higher K_L increases the spontaneity of the adsorption reaction. As a result, it is associated with a more stable adsorbent and more efficient adsorption capacity [44].

Freundlich isotherm model relates to the relationship between the concentration of Cd(II) adsorbed per unit mass of the adsorbent (q_e) and the concentration of the ions in the solution at equilibrium (C_e) [45]. The K_F constant refers to the ability of adsorbents to sorption reactions, and the $1/n$ slope determines the effect of the concentration of metal ions on adsorption capacity. In this study, K_F and n constants were calculated and they are as follows for dosage 2 g/L: (a) 7.98 and 1.58 for CFBC-FA, (b) 9.38 and 1.53 for CFBC-S, respectively. These calculations show that the larger the amount of adsorbent in the sorption reaction, the greater the K_F constant. Therefore, based on the constant values, it can be stated that Cd(II) ions can easily penetrate from aqueous solutions into the surface structure of adsorbent particles. According to the calculated parameters presented in Table 3,

adsorption reactions performed in these studies are more in line with the Freundlich model than with the Langmuir model. The comparison of the maximum adsorption capacity of Cd(II) ions on different adsorbents is shown in Table 4.

5. Conclusions

In this study, CFBC-FA and CFBC-S obtained in one of the municipal wastewater treatment plants in Poland using CFBC technology were used for the removal of Cd(II) ions in adsorption experiments. Firstly, selected physicochemical properties of the adsorbents were characterized using several methods, such as granulation analysis, bulk density, particle size composition, SEM-EDS, thermogravimetry, BET, BJH, SEM, TEM, and FTIR. Secondly, adsorption experiments of cadmium ions were carried out and the influence of such factors on the process efficiency as initial pH, adsorbent dosage, initial concentration of Cd(II) and contact time was examined. As a result, optimal adsorption efficiency of 97.9% (CFBC-FA) and 98.1% (CFBC-S) and experimental adsorption capacity of about 2 mg/g (CFBC-FA and CFBC-S) was observed under following conditions: adsorbent dosage 5 g/L, initial concentration of Cd(II) ions 102.4 mg/L, initial pH 3.9, T = 23°C, contact time 60 min. Overall, as a result of many experiments, it was possible to obtain the efficiency of the adsorption process at the level of over 90%. Thirdly, adsorption kinetics and isotherms analysis was performed. The results indicated that the pseudo-second kinetic model and the Freundlich model better described the examined sorption processes. Based on calculations from the Langmuir equation, the maximum sorption capacity was determined to be 53.19 mg/g (CFBC-FA) and 53.01 mg/g (CFBC-S).

Based on the conducted research, it can be stated that the combustion products obtained as a result of CFBC technology can be successfully used to remove cadmium ions from aqueous solutions. This achievement is undoubtedly an inspiration to continue experiments in this field and maybe a proposal for the potential use of this waste in the processes of removing metals from municipal and industrial wastewater in the future.

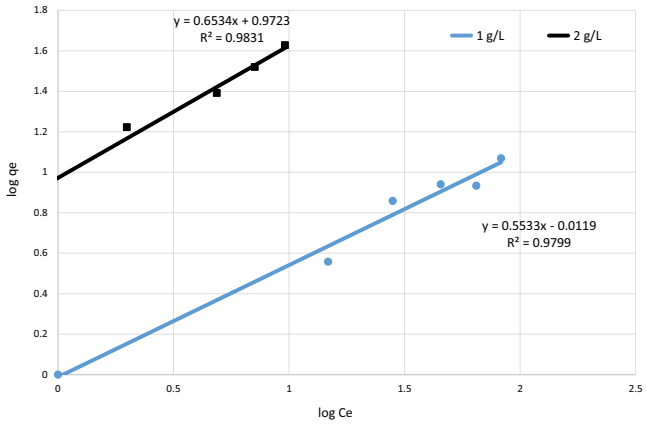

Fig. 19. Freundlich model adsorption isotherms (CFBC-S dosage 1–2 g/L).

Acknowledgments

This research did not receive a specific grant from any funding agency in the public, commercial or not-for-profit sectors. I would like to express special thanks to Dr. Grzegorz Nowaczyk (Nanobiomedical Centre, Adam Mickiewicz University in Poznań, Poland) for taking TEM images on nanoscale of the research samples.

Data availability statement

The data that support the findings of this study are available from the corresponding author upon reasonable request.

Table 4
Comparison of the adsorption capacity of Cd(II) ions using different adsorbents

Adsorbents	q_m (mg/g)
Rice husk [46]	103.09
CFBC-FA (these studies)	53.19
CFBC-S (these studies)	53.01
Clarified sludge [47]	36.23
Sawdust [48]	26.73
Neem bark [48]	25.57
Fired coal fly ash [49]	18.98
Calcite [50]	18.52
Red mud [51]	10.6
Bentonite [52]	9.3
Sawdust [53]	5.37
Bagasse fly ash [54]	2.0

Table 3
Parameters of Langmuir and Freundlich isotherm models

Adsorbent	Adsorbent dosage (g/L)	Langmuir isotherm			Freundlich isotherm		
		Calculated q_m (mg/g)	K_L (L/mg)	R^2	K_F (mg/g)(L/mg)$^{(1/n)}$	n	R^2
CFBC-FA	1	29.97	0.010	0.929	0.980	1.775	0.989
	2	53.19	0.144	0.969	7.983	1.578	0.992
CFBC-S	1	35.14	0.008	0.941	0.973	1.807	0.980
	2	53.01	0.184	0.969	9.383	1.530	0.983

References

[1] A.E. Ofomaja, E.B. Naidoo, S.J. Modise, Removal of copper(II) from aqueous solution by pine and base modified pine cone powder as biosorbent, J. Hazard. Mater., 168 (2009) 909–917.

[2] T. Kalak, A. Kłopotek, R. Cierpiszewski, Effective adsorption of lead ions using fly ash obtained in the novel circulating fluidized bed combustion technology, Microchem. J., 145 (2019) 1011–1025.

[3] WHO, Guidelines for Drinking-Water Quality, Vol. 1., WHO Library Cataloguing-in-Publication Data, Geneva, 2006.

[4] P. Kaewsarn, Q. Yu, Cadmium(II) removal from aqueous solutions by pre-treated biomass of marine alga *Padina* sp., Environ. Pollut., 112 (2001) 209–213.

[5] J.G. Arnason, B.A. Fletcher, A 40+ year record of Cd, Hg, Pb, and U deposition in sediments of Patroon Reservoir, Albany County, NY, USA, Environ. Pollut., 123 (2003) 383–391.

[6] E.I. Unuabonah, K.O. Adebowale, B.I. Olu-Owolabi, L.Z. Yang, L.X. Kong, Adsorption of Pb(II) and Cd(II) from aqueous solutions onto sodium tetraborate-modified Kaolinite clay: equilibrium and thermodynamic studies, Hydrometallurgy, 93 (2008) 1–9.

[7] J.M. Duan, B. Su, Removal characteristics of Cd(II) from acidic aqueous solution by modified steel-making slag, Chem. Eng. J., 246 (2014) 160–167.

[8] Environmental Protection 2014, Statistical Yearbook of GUS, Warsaw, 2015.

[9] AKPGO, Update National Waste Management Plan 2014, Warsaw, 2015.

[10] T. Pająk, Suszenie i spalanie osadów w Polsce i krajach UE. VI Ogólnopolska Konferencja Szkoleniowa: Suszenie i termiczne przekształcanie osadów ściekowych, Warszawa, 2012.

[11] T. Kalak, R. Cierpiszewski, Comparative studies on the adsorption of Pb(II) ions by fly ash and slag obtained from CFBC technology, Pol. J. Chem. Technol., 21 (2019) 72–81.

[12] T. Kalak, K. Marciszewicz, J. Piepiórka-Stepuk, Highly effective adsorption process of Ni(II) ions with the use of sewage sludge fly ash generated by circulating fluidized bed combustion (CFBC) technology, Materials (Basel), 14 (2021) 3106, doi: 10.3390/ma14113106.

[13] T. Kalak, R. Cierpiszewski, M. Ulewicz, High efficiency of the removal process of Pb(II) and Cu(II) ions with the use of fly ash from incineration of sunflower and wood waste using the CFBC technology, Energies, 14 (2021) 1771, doi: 10.3390/en14061771.

[14] T. Kalak, Y. Tachibana, Removal of lithium and uranium from seawater using fly ash and slag generated in the CFBC technology, RSC Adv., 11 (2021) 21964–21978.

[15] K.S. Rao, M. Mohapatra, S. Anand, P. Venkateswarlu, Review on cadmium removal from aqueous solutions, Int. J. Eng. Sci. Technol., 2 (2010) 81–103.

[16] C.W. Cheung, J.F. Porter, G. McKay, Elovich equation and modified second-order equation for sorption of cadmium ions onto bone char, J. Chem. Technol. Biotechnol., 75 (2000) 963–970.

[17] J. Wu, J. Lu, T.H. Chen, Z. He, Y. Su, X. Jin, X.Y. Yao, *In-situ* biotreatment of acidic mine drainage using straw as sole substrate, Environ. Earth Sci., 60 (2010) 421–429.

[18] O. Malerius, J. Werther, Modelling the adsorption of mercury in the flue gas of sewage sludge incineration, Chem. Eng. J., 96 (2003) 197–205.

[19] D. Fytili, A. Zabaniotou, Utilization of sewage sludge in EU application of old and new methods—a review, Renewable Sustainable Energy Rev., 12 (2008) 116–140.

[20] H. Yuansheng, S. Mengshu, What are the environmental advantages of circulating fluidized bed technology?—a case study in China, Energy, 220 (2021) 119711, doi: 10.1016/j.energy.2020.119711.

[21] A. Henclik, J. Kulczycka, K. Gorazda, Z. Wzorek, Conditions of sewage sludge management in Poland and Germany, Inżynieria i Ochrona Środowiska, 17 (2014) 185–197.

[22] B. Nowak, P. Aschenbrenner, F. Winter, Heavy metal removal from sewage sludge ash and municipal solid waste fly ash — a comparison, Fuel Process. Technol., 105 (2013) 195–201.

[23] G. Itskos, N. Koukouzas, C. Vasilatos, I. Megremi, A. Moutsatsou, Comparative uptake study of toxic elements from aqueous media by the different particle-size-fractions of fly ash, J. Hazard. Mater., 183 (2010) 787–792.

[24] S.V. Yadla, V. Sridevi, M.V.V. Chandana Lakshmi, Adsorption performance of fly ash for the removal of lead, Int. J. Eng. Res. Technol., 1 (2012) 1–7.

[25] B. Kostura, R. Dvorsky, J. Kukutschová (Lešková), S. Študentová, J. Bednář, P. Mančík, Preparation of sorbent with a high active sorption surface based on blast furnace slag for phosphate removal from wastewater, Environ. Prot. Eng., 43 (2017) 161–168.

[26] H. Rong, T. Wang, M. Zhou, H. Wang, H. Hou, Y. Xue, Combustion characteristics and slagging during co-combustion of rice husk and sewage sludge blends, Energies, 10 (201) 438, doi: 10.3390/en10040438.

[27] M. Mohebbi, F. Rajabipour, B.E. Scheetz, Reliability of Loss on Ignition (LOI) Test for Determining the Unburned Carbon Content in Fly Ash, 2015 World of Coal Ash (WOCA) Conference in Nasvhille, TN – May 5–7, 2015.

[28] I.J. Alinnor, Adsorption of heavy metal ions from aqueous solution by fly ash, Fuel, 86 (2007) 853–857.

[29] J. Liu, Q. Qiu, F. Xing, D. Pan, Permeation properties and pore structure of surface layer of fly ash concrete, Materials (Basel), 7 (2014) 4282–4296.

[30] Y.-S. Ho, Effect of pH on lead removal from water using tree fern as the sorbent, Bioresour. Technol., 96 (2005) 1292–1296.

[31] C.-H. Weng, C.P. Huang, Adsorption characteristics of Zn(II) from dilute aqueous solution by fly ash, Colloids Surf., A, 247 (2004) 137–143.

[32] L.X. Ma, Q. Wei, Y.Q. Chen, Q.Y. Song, C.H. Sun, Z.Q. Wang, G.H. Wu, Removal of cadmium from aqueous solutions using industrial coal fly ash-nZVI, R. Soc. Open Sci., 5 (2018) 171051, doi: 10.1098/rsos.171051.

[33] W.J. Li, S.Z. Zhou, X.F. Wang, Z. Xu, C. Yuan, Y.C. Yu, Q.Z. Zhang, W.X. Wang, Integrated evaluation of aerosols from regional brown hazes over northern China in winter: concentrations, sources, transformation, and mixing states, J. Geophys. Res., 116 (2011) D015099, doi: 10.1029/2010JD015099.

[34] A. Assi, F. Bilo, A. Zanoletti, J. Ponti, A. Valsesia, R. La Spina, L.E. Depero, E. Bontempi, Review of the reuse possibilities concerning ash residues from thermal process in a medium-sized urban system in Northern Italy, Sustainability, 12 (2020) 4193, doi: 10.3390/su12104193.

[35] M. Martínez, N. Miralles, S. Hidalgo, N. Fiol, I. Villaescusa, J. Poch, Removal of lead(II) and cadmium(II) from aqueous solutions using grape stalk waste, J. Hazard. Mater., 133 (2006) 203–211.

[36] Z. Kavaliauskas, V. Valincius, G. Stravinskas, M. Milieska, N. Striugas, J. The investigation of solid slag obtained by neutralization of sewage sludge, J. Air Waste Manage. Assoc., 65 (2015) 1292–1296.

[37] S. Ueda, H. Koyo, T. Ikeda, Y. Kariya, M. Maeda, Infrared emission spectra of CaF_2-CaO-SiO_2 melt, ISIJ Int., 40 (2000) 739–743.

[38] O. Iliashevsky, E. Rubinov, Y. Yagen, M. Gottlieb, Functionalization of silica surface with UV-active molecules by multivalent organosilicon spacer, Open J. Inorg. Chem., 6 (2016) 163–174.

[39] X.Q. Cui, S.Y. Fang, Y.Q. Yao, T.Q. Li, Q.J. Ni, X. Yang, Z.L. He, Potential mechanisms of cadmium removal from aqueous solution by *Canna indica* derived biochar, Sci. Total Environ., 562 (2016) 517–525.

[40] I. Mobasherpour, E. Salahi, M. Pazouki, Comparative of the removal of Pb^{2+}, Cd^{2+} and Ni^{2+} by nano crystallite hydroxyapatite from aqueous solutions: adsorption isotherm study, Arabian J. Chem., 5 (2012) 439–446.

[41] V. Mînzatu, C.-M. Davidescu, P. Negrea, M. Ciopec, C. Muntean, I. Hulka, C. Paul, A. Negrea, N. Duteanu, Synthesis, characterization and adsorptive performances of a composite material based on carbon and iron oxide particles, Int. J. Mol. Sci., 20 (2019) 1609, doi: 10.3390/ijms20071609.

[42] N.S. Langeroodi, Z. Farhadravesh, A.D. Khalaji, Optimization of adsorption parameters for Fe(III) ions removal from aqueous solutions by transition metal oxide nanocomposite, Green Chem. Lett. Rev., 11 (2018) 404–413.
[43] Y.S. Ho, G. McKay, Pseudo-second-order model for sorption processes, Process Biochem., 34 (1999) 451–465.
[44] S.B. Wang, E. Ariyanto, Competitive adsorption of malachite green and Pb ions on natural zeolite, J. Colloid Interface Sci., 314 (2007) 25–31.
[45] P. Senthil Kumar, C. Vincent, K. Kirthika, K. Sathish Kumar, Kinetics and equilibrium studies of Pb^{2+} ion removal from aqueous solutions by use of nano-silversol-coated activated carbon, Braz. J. Chem. Eng., 27 (2010) 339–346.
[46] M. Ajmal, R.A.K. Rao, S. Anwar, J. Ahmad, R. Ahmad, Adsorption studies on rice husk: removal and recovery of Cd(II) from wastewater, Bioresour. Technol., 86 (2003) 147–149.
[47] T.K. Naiya, A.K. Bhattacharya, S.K. Das, Removal of Cd(II) from aqueous solutions using clarified sludge, J. Colloid Interface Sci., 325 (2008) 48–56.
[48] T.K. Naiya, P. Chowdhury, A.K. Bhattacharya, S.K. Das, Sawdust and neem bark as low-cost natural biosorbent for adsorptive removal of Zn(II) and Cd(II) ions from aqueous solutions, Chem. Eng. J., 148 (2009) 68–79.
[49] A. Papandreou, C.J. Stournaras, D. Panias, Copper and cadmium adsorption on pellets made from fired coal fly ash, J. Hazard. Mater., 148 (2007) 538–547.
[50] Ö. Yavuz, R. Guzel, F. Aydin, I. Tegin, R. Ziyadanogullari, Removal of cadmium and lead from aqueous solution by calcite, Pol. J. Environ. Stud., 16 (2007) 467–471.
[51] E. López, B. Soto, M. Arias, A. Núñez, D. Rubinos, M.T. Barral, Adsorbent properties of red mud and its use for wastewater treatment, Water Res., 32 (1998) 1314–1322.
[52] M. Ulmanu, E. Marañón, Y. Fernández, L. Castrillón, I. Anger, D. Dumitriu, Removal of copper and cadmium ions from diluted aqueous solutions by low cost and waste material adsorbents, Water Air Soil Pollut., 142 (2003) 357–373.
[53] Y. Bulut, Z. Tez, Removal of heavy metals from aqueous solution by sawdust adsorption, J. Environ. Sci., 19 (2007) 160–166.
[54] V.K. Gupta, C.K. Jain, I. Ali, M. Sharma, V.K. Saini, Removal of cadmium and nickel from wastewater using bagasse fly ash—a sugar industry waste, Water Res., 37 (2003) 4038–4044.

Supplementary information

S1. Methods of circulating fluidized bed combustion fly ash and slag characterization

In the research, circulating fluidized bed combustion fly ash (CFBC-FA) and slag (CFBC-S) particles with a diameter in the range of 0–0.212 mm were used. Firstly, physico-chemical properties of the materials were analyzed using several methods, including:

(1) Determination of granulation was performed by a sieve method in accordance with the standard PN-C-97555-01:1988P. In order to separate individual ash fractions, they were screened through four sieves with mesh diameters of 0.212 to 1.0 mm over 1 h. Fractions retained on individual

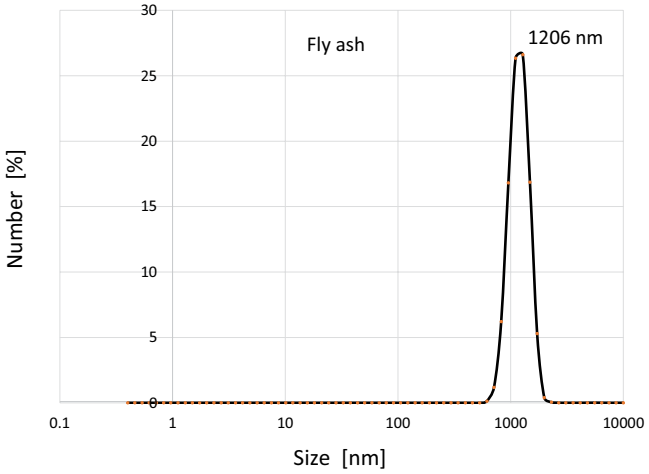

Fig. S1. A plot of the particle size distribution of CFBC fly ash.

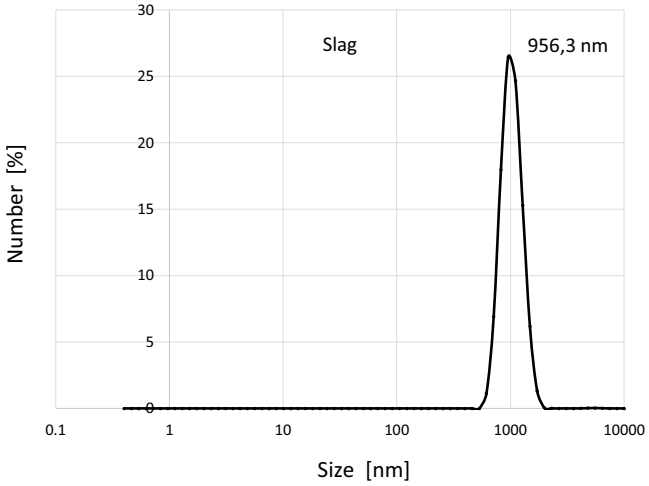

Fig. S2. A plot of the particle size distribution of CFBC slag.

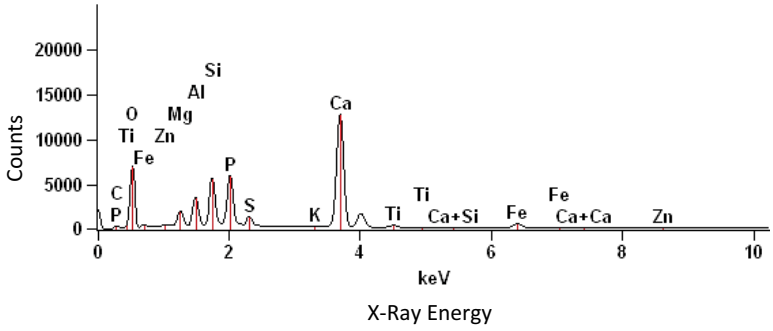

Fig. S3. EDS spectrum of CFBC fly ash (Magn.: x200).

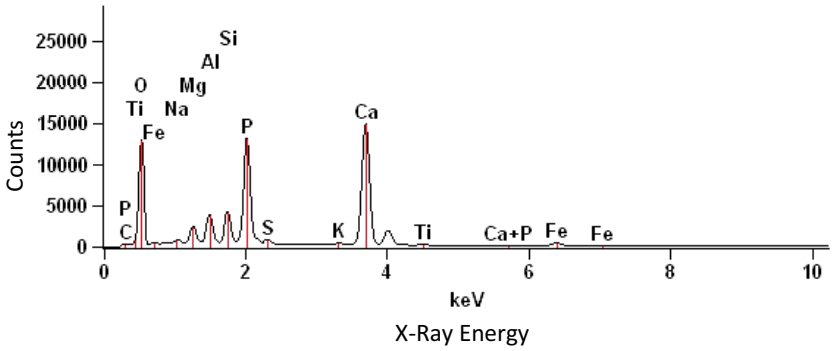

Fig. S4. EDS spectrum of CFBC slag (Magn.: x200).

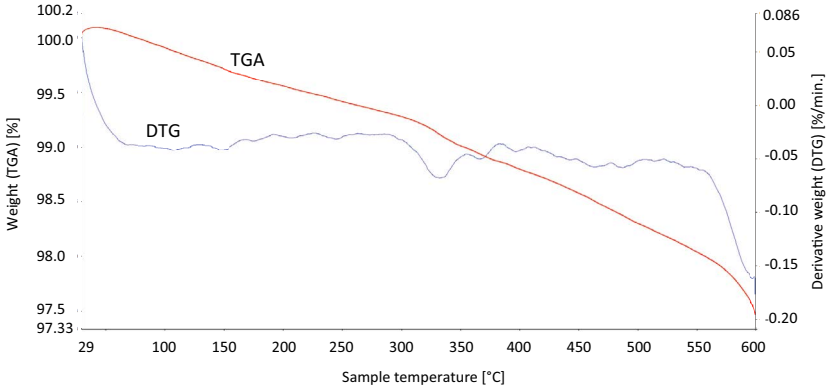

Fig. S5. Thermogravimetric curves of CFBC fly ash.

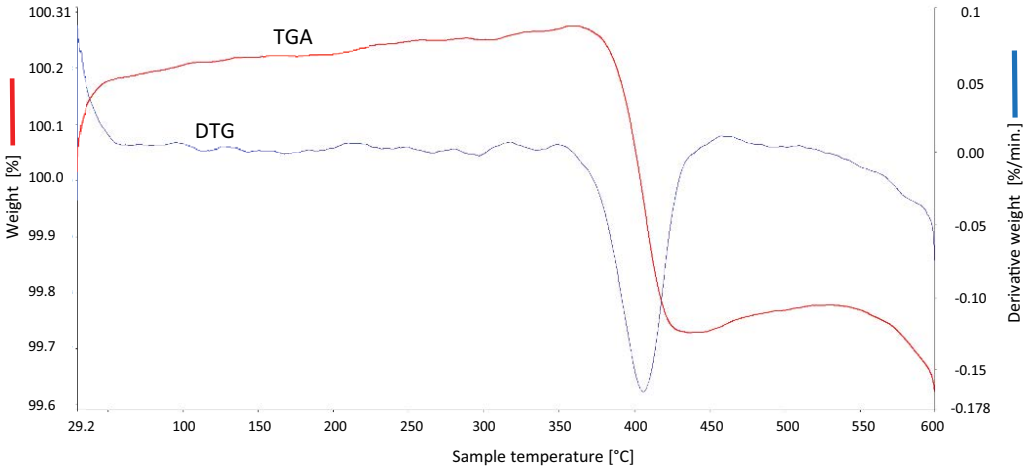

Fig. S6. Thermogravimetric curves of CFBC slag.

sieves were weighed and the procedure was performed in triplicate. The main composition was the percentage content of particles of a certain diameter (grain faction, X (%)) was calculated according to Eq. (S1).

$$X = \frac{m_1}{m_2} \times 100\% \quad \text{(S1)}$$

where: m_1 (g) is the mass of sifted material and m_2 (g) is the initial mass of a sample.

(2) Determination of particle size distribution was performed by the laser diffraction method using a Zetasizer Nano ZS (Malvern Instruments Ltd., United Kingdom), which is capable of measuring powders with a size distribution ranging from 0.2 to 2,000 μm.

(3) Determination of bulk density was performed according to the standard PN-S-96035:1997. The mass and volume of fly ash were determined using a measuring cylinder. Measurements were repeated six times. Bulk density X (g/cm^3) was calculated according to Eq. (S2).

$$X = \frac{m_1 - m_0}{V} \quad \text{(S2)}$$

where: m_1 (g) is the mass of a cylinder with fly ash; m_0 (g) is the mass of an empty cylinder and V (cm^3) is the volume of fly ash in a cylinder.

(4) The elemental composition and mapping of fly ash samples were examined with a scanning electron microscopy (SEM) Hitachi S-3700N (Hitachi High-Technologies Corporation, Tokyo, Japan) with an attached a Noran SIX energy-dispersive X-ray spectrometer (EDS) microanalyzer (ultradry silicon drift type with resolution (FWHM) 129 eV, accelerating voltage: 20.0 kV).

(5) Thermal stability was determined by thermogravimetric analysis using the apparatus Setsup DTG, DTA 1200 (Setaram, KEP Technologies EMEA, Caluire, France). Fly ash samples were heated at the speed of 10°C/min. in the temperature range 30°C–1,000°C under a nitrogen atmosphere at a flow rate of 20 mL/min.

(6) The specific surface area and the average pore diameter were determined with the Brunauer–Emmett–Teller (BET) method using Autosorb iQ Station 2 (Quantachrome Instruments, USA).

(7) The pore volume was determined by Barrett–Joyner–Halenda (BJH) method using Autosorb iQ Station 2 (Quantachrome Instruments, USA).

(8) The morphology of the fly ash samples was examined with a SEM EVO-40 (Carl Zeiss, Germany).

(9) The surface structure of fly ash was examined in infrared spectroscopy using a Fourier-transform attenuated total reflection (FTIR-ATR) Spectrum 100 (PerkinElmer, Waltham, USA).

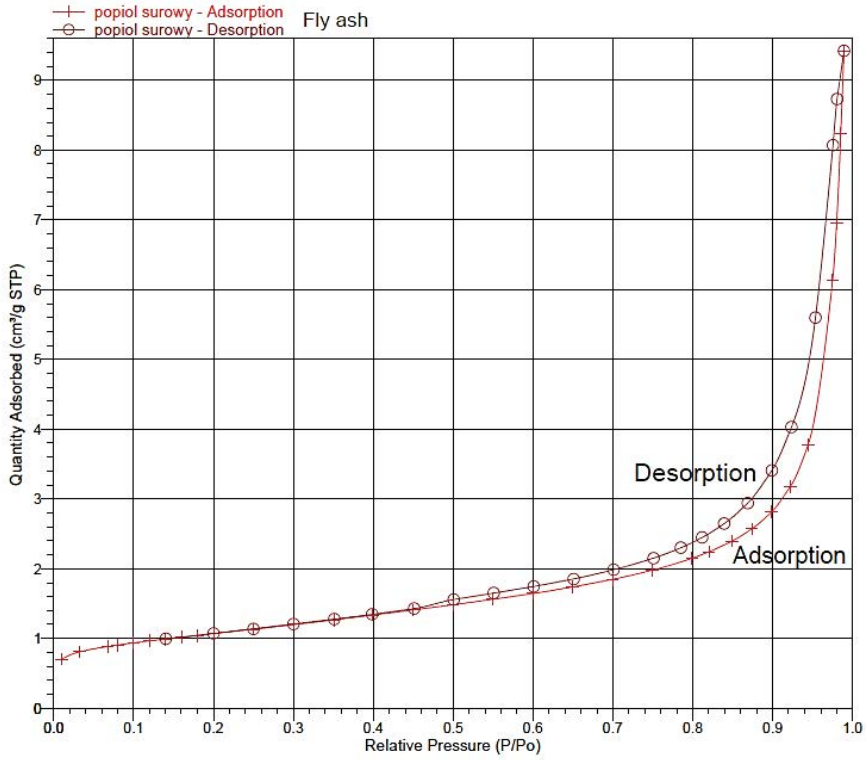

Fig. S7. The low-temperature BET adsorption and desorption isotherms of CFBC fly ash.

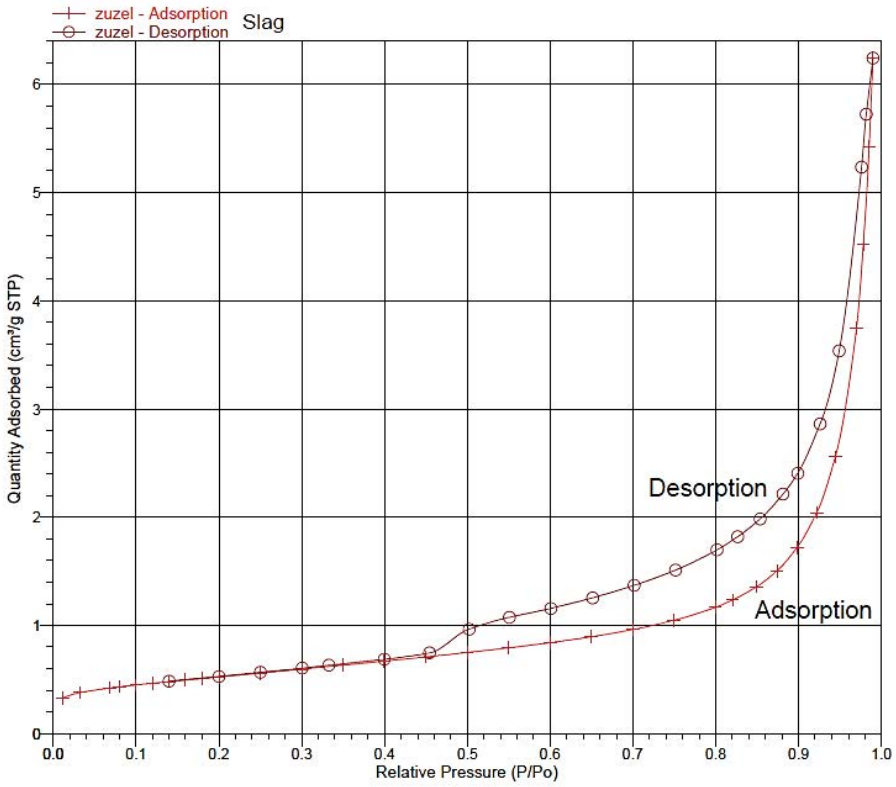

Fig. S8. The low-temperature BET adsorption and desorption isotherms of CFBC slag.

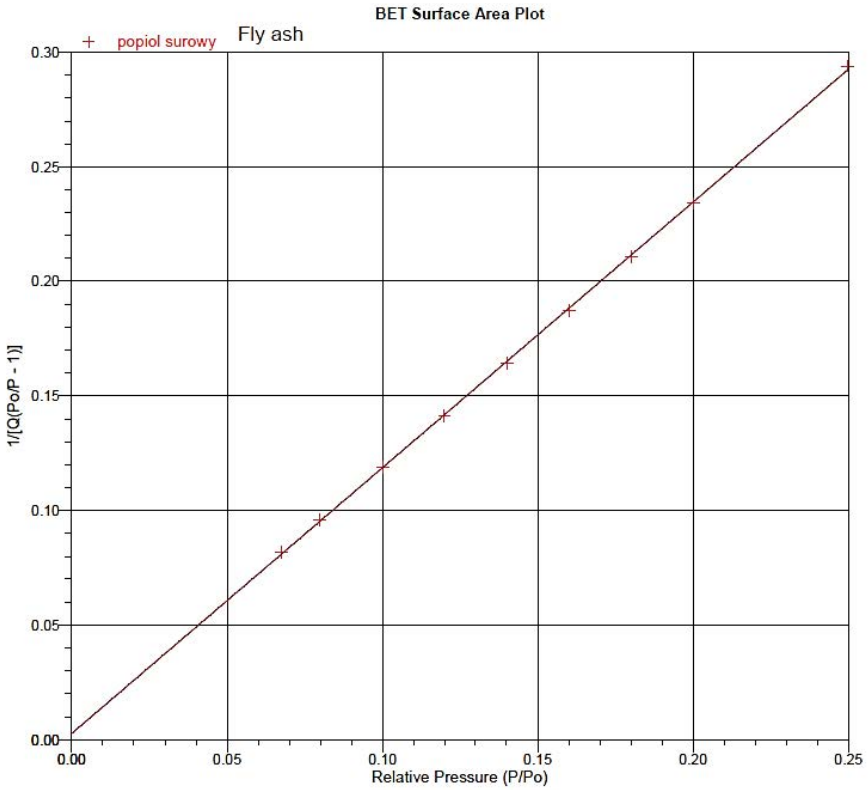

Fig. S9. Linear BET isotherm of CFBC fly ash.

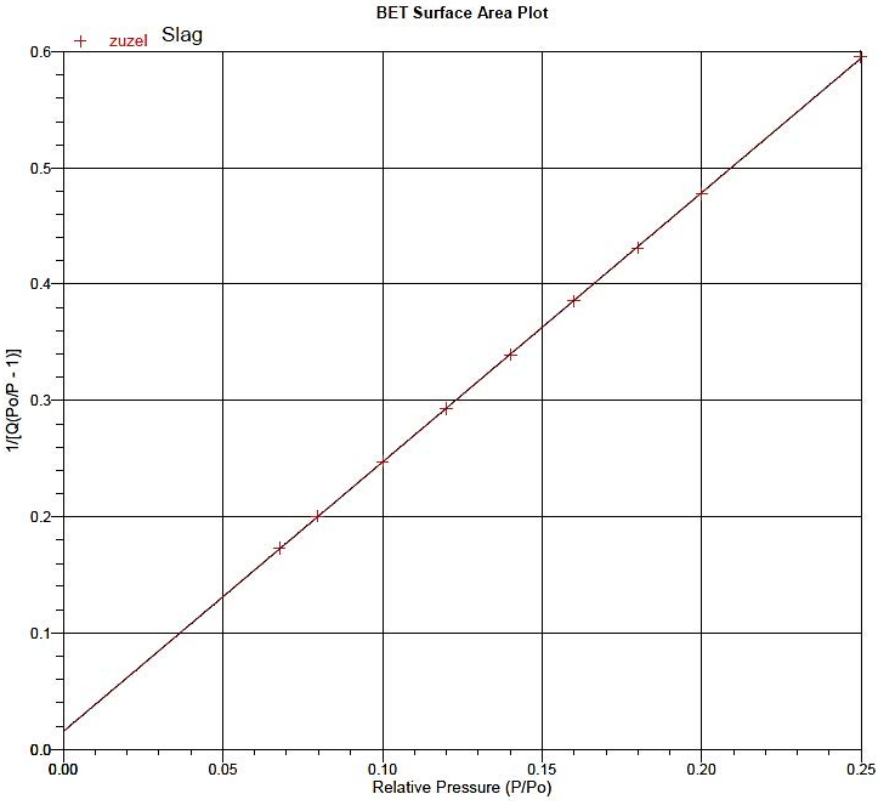

Fig. S10. Linear BET isotherm of CFBC slag.

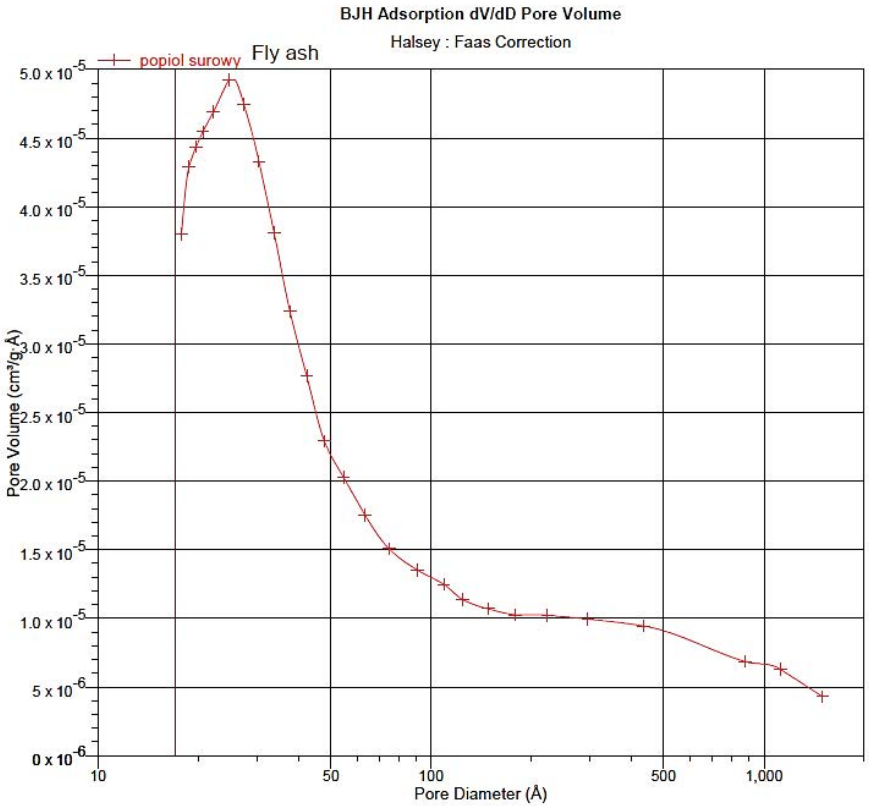

Fig. S11. BJH adsorption isotherm of CFBC fly ash.

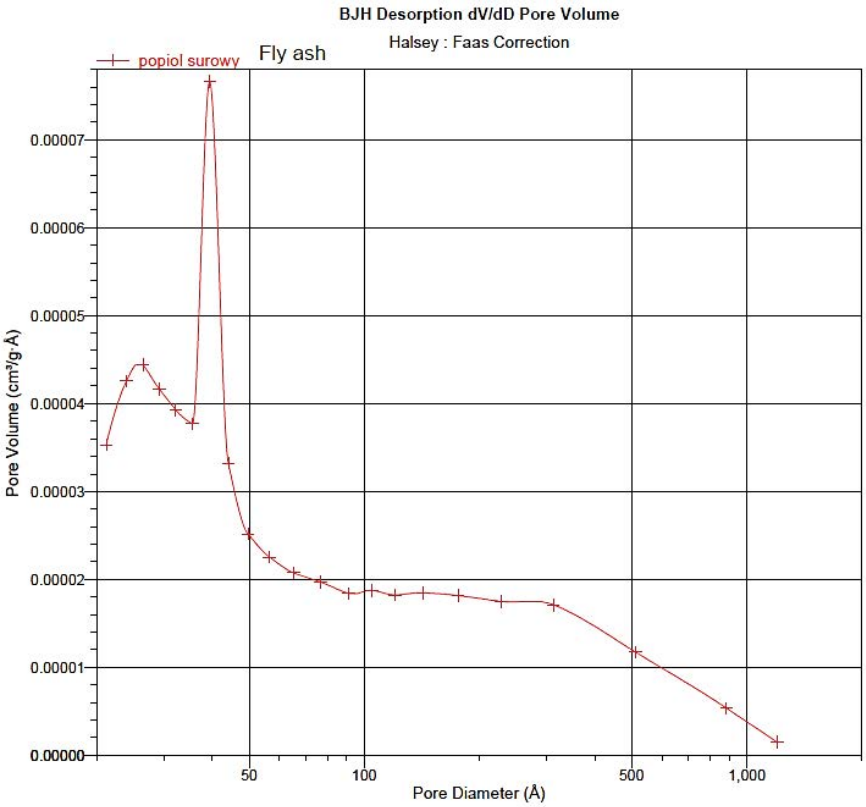

Fig. S12. BJH desorption isotherm of CFBC fly ash.

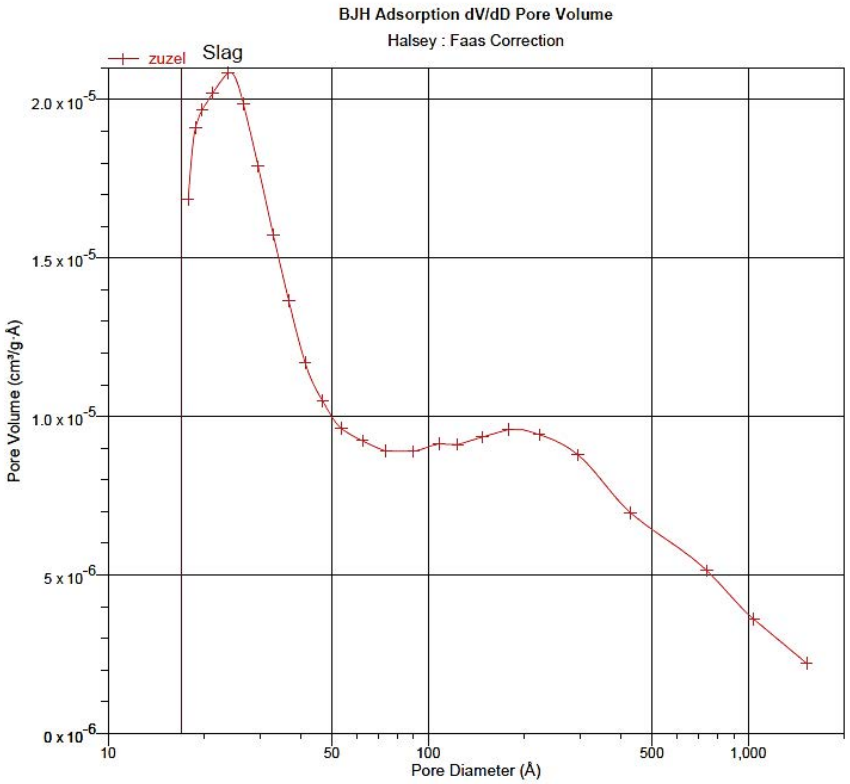

Fig. S13. BJH adsorption isotherm of CFBC slag.

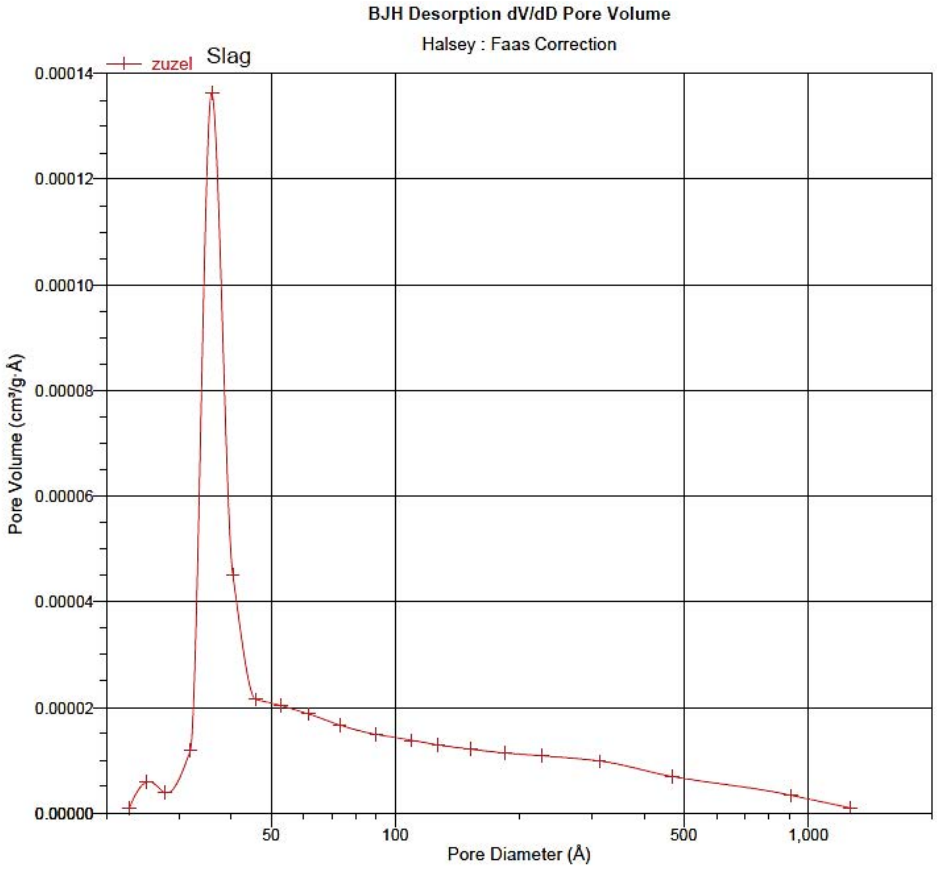

Fig. S14. BJH desorption isotherm of CFBC slag.

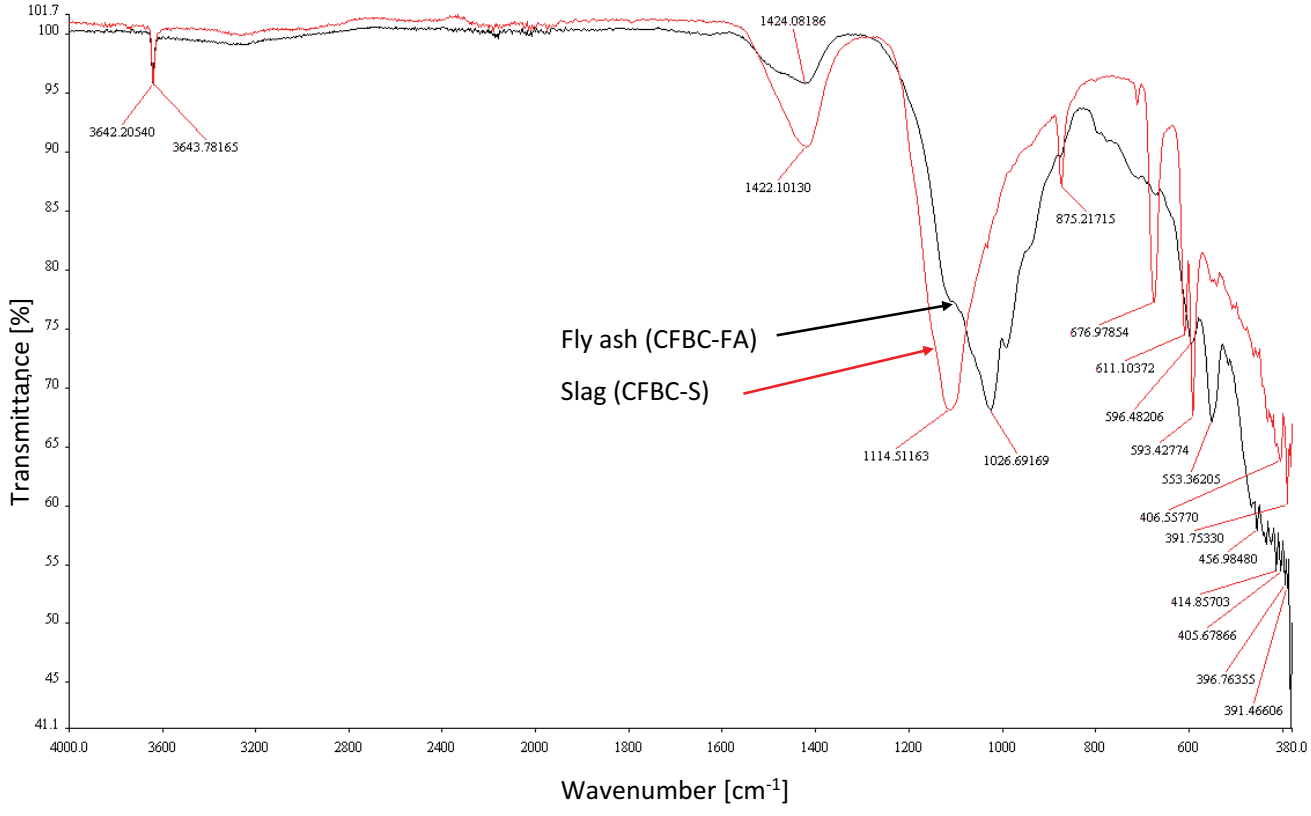

Fig. S15. FTIR spectrum of CFBC-FA and CFBC-S.